The ROYAL COLLEGE *of* OPHTHALMOLOGISTS

ARTICLE

Retinal and circumpapillary nerve fiber layer thickness and associated factors in children

Yao Yao [1] · Jing Fu [1] · Lei Li[1] · Weiwei Chen[1,2] · Zhaojun Meng[1] · Han Su [1] · Wei Dai[1]

Abstract

Objective To evaluate the distribution of macula and circumpapillary retina nerve fiber layer (cpRNFL) thickness and other associated factors among grade-1 primary school children in Lhasa using spectral-domain optical coherence tomography (SD-OCT).

Methodology OCT assessment was conducted on 1856 grade-1 students from 7 primary schools in Lhasa, Tibet following a successful random stratified sampling of the students. Each child underwent comprehensive general and ocular examinations as well as an SD-OCT detection (12×9 mm, 3D wide scan mode, Topcon 3D OCT-1) to assess the thickness of the macula, ganglion cell-inner plexiform layer (GCIPL), ganglion cell complex (GCC), and cpRNFL. Multivariate and correlation analyses were performed to evaluate the association of the demographic and ocular variables.

Results The average age of the 1762 (94.43%) students who underwent OCT assessment was 6.83 ± 0.46 years. Among them, 984 (53.02%) were boys. The number of students who had macular, cpRNFL, and optic disc scans completed and with adequate image quality were 1412 (82.2%), 1277 (74.4%), and 1243 (72.4%), respectively. The average macula full retinal thickness (FRT), GCIPL, GCC, and cpRNFL thickness of the students was 279.19 ± 10.61 μm, 76.41 ± 4.70 μm, 108.15 ± 6.15 μm, and 112.33 ± 13.5 μm, respectively. Multivariate regression and correlation analysis further revealed that boys and girls had significant differences in their average cpRNFL thickness. Moreover, GCC and GCIPL thickness was negatively correlated with IOP but positively correlated with the body mass index. The thickness of all the layers of the macula and cpRNFL were positively correlated with spherical equivalent. Further to this, the average macular FRT, GCIPL, and GCC thicknesses were positively correlated with cpRNFL global thickness.

Conclusion This study describes the normal distribution of macular retina, cpRNFL, and optic disc parameters in grade-1 Tibetan children in Lhasa. It contributes to the establishment of a normative ophthalmology database of Tibetan children, and advances the ability of OCT in ophthalmic disorder diagnosis during long-term monitoring in plateau.

Background

Vision screening for children is fundamental to detect reduced visual acuity and risk factors that threaten vision

✉ Jing Fu
fu_jing@126.com

1 Beijing Tongren Eye Center, Beijing Tongren Hospital, Capital Medical University, Beijing Key Laboratory of Ophthalmology & Visual Sciences, Beijing, China

2 Beijing Institute of Ophthalmology, Beijing, China

impairment or blindness. Cerebral visual impairment and optic nerve anomalies remain the major causes of severe vision loss in high-income countries. On the contrary, retinopathy of prematurity (ROP), cataracts, corneal conditions caused by infectious diseases, and amblyopia commonly affect the healthy growth and development of the eye and visual systems in low- and middle-income countries [1] Early childhood periodic ocular assessment is an important method for screening latent and early symptomatic ocular disorders. In addition, a combined series of screening methods that include objective and quantified measurements of visual functions and structure changes are highly significant because they have high accuracy and reliability in assessing children's ocular health [2].

Optical coherence tomography (OCT) is a non-invasive technology that has significantly altered the understanding

and management of serial ocular disorders. The technology enables in vivo quasi-histological evaluation that provides high-resolution cross-sectional images of the retina, retinal nerve fiber layer, and the optic nerve head. This further reveals the subtle subclinical changes of the retina [3]. Moreover, OCT can accurately and quantitatively measure the hierarchical structure of the retina during disease development. For example, SD-OCT revealed that thinning of circumpapillary RNFL (cpRNFL) is related to decreased visual function such as hypoplasia of optic nerve, congenital glaucoma, optic neuritis, and autosomal dominant optic atrophy in children. Changes in macular thickness are also associated with those factors [4–8]. It is also postulated that retinal ganglion cell-related structures such as the thickness of ganglion cell-inner plexiform layer (GCIPL), ganglion cell complex (GCC) are also related to glaucoma and various optic nerve diseases [9–11]. Cognizant to this, combining OCT with advanced computer techniques such as machine learning can significantly expand the understanding of ocular impairments.

In recent years, OCT has displayed its superiority over fundus photography in vision screening programs [12, 13]. However, most previous studies were limited to observing only specific regions of the retina such as the optic disc or macular area [14–17]. Although developmental biology shows that there are correlations between ganglion axons, retinal layers, and optic nerve formation, the sensitivity of assessing different retinal diseases from separate parts still needs verification [18]. Moreover, the thickness of the macular area at different levels is an indicator of the existence of other eye diseases. It is, therefore, necessary to conduct a comprehensive examination of each area of the retina, and evaluate the correlation between retinal, circumpapillary, and optic disc parameters. Herein, a spectral-domain OCT was employed to evaluate the thickness of cpRNFL, macular full retina, GCC, GCIPL, and optic disc-related parameters simultaneously. This eliminated repetitive measurement errors and contributed to the comprehensive evaluation and correlation analysis of different levels and positions of the retina.

To date, there is no ocular information database for Tibetan children. Cognizant to this, this study aimed to evaluate macular FRT, GCIPL, GCC, circumpapillary RNFL thickness, and optic disc parameters in Tibetan children using SD-OCT. The Tibetan Plateau has a high altitude as well as sufficient sunshine. It is inhabited by a variant of ethnic groups. Environmental factors such as climate and light as well as different eating habits and other factors can potentially influence differential eye development in children. This led to the set-up of the school-based Lhasa Childhood Eye Study (LCES). It was an observational vision screening study with a long-term follow-up time. The findings of this study complement the existing understanding of pediatric ocular conditions and advance the ability of OCT in vision screening among children.

Materials and methods

Study population and design

The Lhasa Childhood Eye Study (LCES) was a school-based, observational cohort epidemiological study on childhood ocular diseases. The study protocols were in accordance with the declaration of Helsinki. It was also approved by the Ethics Committee of the Beijing Tongren Hospital, Capital Medical University (No. TRECKY2019-058). All participants' parents or legal guardians gave written informed consent prior to the study. The LCES employed the stratified cluster sampling method to sample grade one students in Lhasa, Tibet, southwest of China. Based on local government evaluations, 27 out of 28 elementary schools in Lhasa that effectively participated in the LCES were stratified into three levels. Consequently, 7 elementary schools with 1942 grade-1 students were selected. The study continued for 5 years till the students got to junior high school.

Study protocols and examination methods

All students underwent a comprehensive eye examination that included assessment of uncorrected and best-corrected visual acuity (BCVA), stereopsis acuity (S0001, STEREO, USA), ocular dominance, slit-lamp bio-microscopy evaluation (SL-3G, Topcon, Tokyo, Japan), non-contact tonometry (CT-800, Topcon, Tokyo, Japan), ocular alignment, objective refraction measurement before and after cycloplegia, OCT, and taking of retinal photographs.

Myopia and hyperopia were defined as ≤ -0.50 diopters (D) SE and $\geq +2.00D$ SE, respectively, in one or both eyes. In addition, body height and weight, blood oxygen saturation, and heart rate were also measured and recorded as anthropometric parameters. The body mass index (BMI) of the patients was calculated by dividing the patient's weight (kg) by the square of his height (m) (kg/m^2). Blood oxygen saturation and the heart rate of patients were measured twice using a digital fingertip pulse oximeter. Their average values were then used for statistical analysis.

OCT measurements

OCT examination was performed by an experienced technician using a spectral-domain OCT (3D OCT-1, Topcon, Tokyo, Japan). Topcon 3D OCT-1 is a non-contact SD-OCT system that performs a fully automated "alignment, focus, and capture" procedure by capturing 50,000 axial
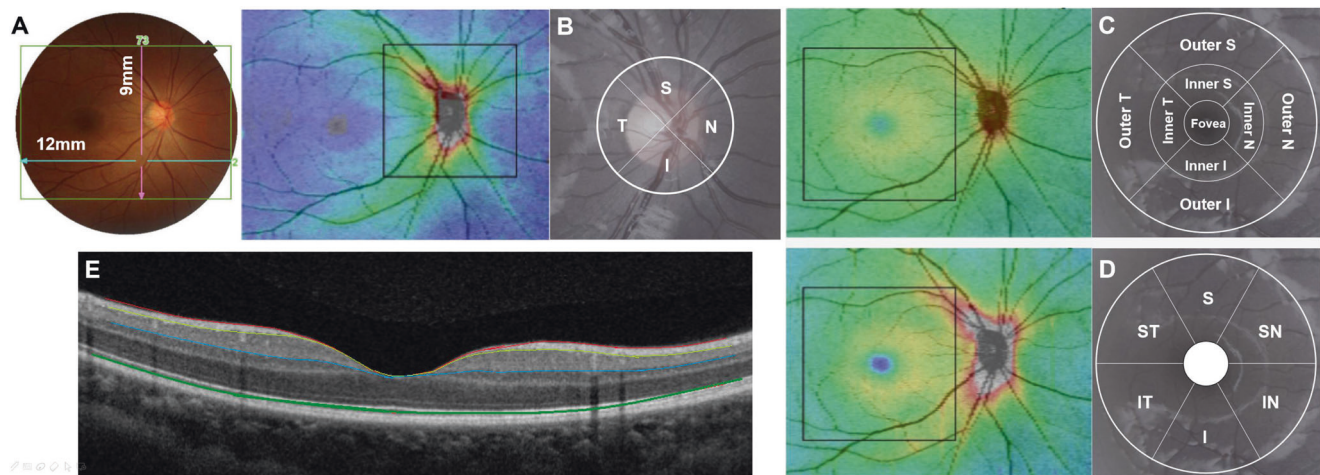
Fig. 1 The OCT measurements. The 12×9 mm scan region (**A**). Measurement areas for cpRNFL circle (**B**). Macula ETDRS grid (**C**), macula 6 circle for GCIPL, and GCC (**D**) overlaid with example projected images. Full retinal thickness (distance between the red and green boundaries); ganglion cell + inner plexiform layers (distance between the yellow and blue boundaries); ganglion cell complex (distance between the red and blue boundaries, vitreal to inner nuclear layer) (**E**). All the images were set with the right eye orientation.

scans per second [19]. Herein, the "3D wide scan mode" was selected to provide a 12 mm × 9 mm scan measurement and topographical maps of the optic nerve and macula (Fig. 1a). The mode also featured an automatic segmentation of RNFL, total retina, GCIPL, and GCC (Fig. 1b–d, e).

The macula full retinal thickness (FRT) was defined as the distance between the inner limiting membrane (ILM) and the outer segments/retinal pigment epithelium junction boundary. It was divided into nine quadrants based on the ETDRS map (Fig. 1c). The diameters of the three circles on the ETDRS map are 1, 3, and 6 mm. In the same line, GCIPL thickness was defined as the distance from the interface between the NFL and ganglion cell layer (GCL) to the interface between the inner plexiform layer (IPL) and inner nuclear layer (INL). GCC was defined as the distance between the internal limiting membrane and the interface between the IPL and INL. It was the sum of RNFL and GCIPL (Fig. 1e). The temporal-superior-nasal-inferior-temporal (TSNIT) circle with a diameter of 3.4 mm was placed automatically at the optic disc center to obtain the optic nerve head parameters. The thickness of cpRNFL was assessed over 4 quadrants and 12 clock-hour sectors around the TSNIT circle (Fig. 1b). The optic disc contour was automatically detected. However, the disc area, cup area, rim area, cup/disc (C/D) vertical diameter, C/D area, cup volume, and rim volume were measured.

Only images that met the required criteria were included in subsequent analysis. Children whose images had a low signal, blinks, or motion artifacts were excluded from the study. This was also the case for children who had undergone intraocular surgeries or pathologies to fix ptosis or remove congenital cataracts. Children who had difficulties in cooperating with the test were also excluded from the study. All the collected images were examined for any automatic segmentation errors on foveal centration, boundary segmentations, or disc margin with a fast map. When such errors were detected, manual adjustments were performed based on the anatomy of the eyes, and the adjustment electronically documented [14, 16]. The children's healthy right eyes were chosen for evaluation [17, 20].

Statistical analysis

Values for the continuous variables were presented as means ± standard deviation and as percentages for categorical variables. Data were analyzed using the Statistical Analysis System software (version 9.4, SAS Inc, Cary, NC, USA). Correlation analysis was used to calculate the correlation coefficient between RNFL thickness and C/D ratio, as well as the ratio between macular FRT, GCC, GCIPL, and RNFL thickness. Covariance analyses were used to evaluate gender-based differences. In these analyses, adjustments of multiple variables were also done. Multivariate regression analyses were used to assess the effect of gender, height, body mass index (BMI), intraocular pressure (IOP), blood oxygen saturation, and refractive error on the retina thickness.

Results

Study population and general characteristics

OCT assessment was conducted on 1856 participants enrolled in the study. Among the 1856 participants, 170

participants were excluded for varying reasons; 153 participants failed to complete protocols and/or examination procedures while 17 had ocular diseases (Supplementary Fig. 1). This resulted into an analyzable fraction of 90.8%. The average age of students who underwent OCT assessment was 6.83 ± 0.46 years. Among them, 53.02% were boys while 46.98% were girls. The participants were comprised of 94.93% of Tibetan minority children. The average BMI, blood oxygen saturation, and IOP of the participants was $15.74 \pm 1.80 \, \mathrm{kg/m^2}$, $92.7 \pm 3.7\%$, and $16.02 \pm 2.73 \, \mathrm{mmHg}$, respectively. Moreover, the average cycloplegic SE of the participants was $+1.07 \pm 0.92\mathrm{D}$ because 10.78% of the participants had refractive errors.

After manual screening of the different OCT scan positions and image quality, the number of students who had macular, cpRNFL and optic disc scans completed, and with adequate image quality was 1412 (82.2%), 1277 (74.4%), and 1243 (72.4%), respectively. The characteristics of the included and excluded groups (participants) are shown in Table 1. There were no significant ethnic differences or bias between the two groups. However, the number of boys in the exclusion group was significantly higher than that of girls in all three scans.

Thickness and distributions of macular FRT, GCIPL, and GCC

Supplementary Table 1 shows the thickness and distribution data of macular FRT, GCIPL, and GCC. The average thickness of macular FRT, GCIPL, and GCC was $279.19 \pm 10.61 \, \mu\mathrm{m}$, $76.41 \pm 4.70 \, \mu\mathrm{m}$, and $108.15 \pm 6.15 \, \mu\mathrm{m}$, respectively (Fig. 2a). The superior region ($305.64 \pm 12.07 \, \mu\mathrm{m}$) of the inner circle of macular FRT was the thickest area. It was followed by the inferior, nasal, and temporal regions, respectively, without any significant differences across regions. Nonetheless, the outer ring of the nasal region ($295.36 \pm 13.17 \, \mu\mathrm{m}$) was significantly thicker than the temporal ($P < 0.01$), superior ($P < 0.01$), and inferior ($P < 0.01$) regions (data not shown in tables).

RNFL thickness, distribution, and optic disc parameters

The overall cpRNFL thickness and distribution are shown in Supplementary Table 1. The average cpRNFL thickness was $112.86 \pm 11.94 \, \mu\mathrm{m}$. The thickest area was the inferior region ($146.99 \pm 19.13 \, \mu\mathrm{m}$), followed by the superior ($144.90 \pm 17.60 \, \mu\mathrm{m}$), the temporal ($79.99 \pm 12.88 \, \mu\mathrm{m}$), and the nasal quadrants ($79.51 \pm 16.00 \, \mu\mathrm{m}$). The thickness and distribution of the 12 individual sections (each section was $30°$, corresponding to a clock-wised hour) were also different. The thickest region was in the 6 o'clock section ($162.11 \pm 28.15 \, \mu\mathrm{m}$), while the thinnest was in the 3 o'clock section ($61.56 \pm 14.79 \, \mu\mathrm{m}$). However, the cpRNFL thickness of the 12 sections was more discrete than that of the 4 regions (Inferior, superior, temporal, and nasal) (Supplementary Table 2 and Fig. 2b).

The basic statistical parameters of the optic disc variables are shown in Supplementary Table 1. The average disc and cup area were 2.8 ± 0.41 and $0.86 \pm 0.51 \, \mathrm{mm^2}$ with an average cup/disc ratio (CDR) of 0.3 ± 0.15. The disc was oval-shaped based on its vertical and horizontal diameters.

Factors influencing the thickness of macular FRT, GCIPL, GCC, and cpRNFL, and optic disc parameters

The average thickness of the macula FRT of the boys and the girls was not significantly different ($P = 0.31$). However, the average thickness of their inner circle regions was significantly different ($P < 0.01$) (Supplementary Table 2). In the same line, multivariate regression analysis revealed that macular FRT was significantly correlated with SE ($P < 0.01$). In addition, the thickness of GCIPL and GCC was correlated with SE, IOP, and BMI (Table 2). However, the thickness of the macular retina of each layer and region of the hyperopic, myopic, and emmetropic patients (groups) was not significantly different (Supplementary Table 3).

The average RNFL thickness between the boys and the girls was significantly different ($P < 0.01$). This was particularly the case in the inferior ($P < 0.01$) and superior regions ($P < 0.05$) (Supplementary Table 4). Univariate linear regression analysis further revealed that RNFL thickness had a significant positive correlation with positive SE ($P < 0.01$) and female participants ($P < 0.01$). However, there were no significant correlations between RNFL thickness and ethnicity ($P = 0.62$), age ($P = 0.06$), height ($P = 0.77$), BMI ($P = 0.28$), blood oxygen saturation ($P = 0.56$), and IOP ($P = 0.21$) (Table 2). Moreover, there were no significant differences in the average RNFL thickness between the hyperopic, myopic, and emmetropic participants (groups) (Supplementary Table 5). Only the nasal quadrant region showed a significant difference in RNFL thickness when separated by TSIN regions ($P = 0.02$).

The optical disc area and rim area had a significant correlation with cpRNFL thickness (Fig. 3a). However, the correlation of the CDR < 0.5 group and CDR ≥ 0.5 group with cpRNFL thickness was not significantly different.

Correlation analysis between cpRNFL and macular FRT, GCIPL and GCC thickness

The thickness of cpRNFL was positively correlated with that of macular FRT ($R^2 = 0.113$, $P < 0.001$), GCC ($R^2 = 0.0503$, $P < 0.001$), and GCIPL ($R^2 = 0.447$, $P < 0.001$). Moreover, the retinal thickness of each layer is was found to be related to the SE. Figure 3b–d shows three-dimensional

Table 1 Characteristics of children with and without scans of the macular, RNFL, and optic disc in the LCES study.

	Complete macular scans			Complete RNFL scans			Complete optic disc scans		
	Included $n = 1412$	Excluded $n = 444$	P-value	Included $n = 1277$	Excluded $n = 579$	P-value	Included $n = 1243$	Excluded $n = 613$	P-value
Ethnicity (n, %)									
Tibetan	1341 (95.0%)	421 (94.8%)		1208 (94.6%)	554 (95.7%)		1174 (94.4%)	588 (96.0%)	
Han	64 (4.5%)	21 (4.7%)	0.98	63 (4.9%)	22 (3.8%)	0.55	63 (5.1%)	22 (3.6%)	0.34
Other	7 (0.5%)	2 (0.5%)		6 (0.5%)	3 (0.5%)		6 (0.5%)	3 (0.4%)	
Sex (boys, %)	719 (53.6%)	265 (62.9%)	<0.001[b]	653 (54.1%)	331 (59.7%)	0.02[b]	632 (53.8%)	352 (59.8%)	<0.001[b]
Height (cm)[a]	120.61 (120.32–120.90)	120.35 (119.83–120.86)	0.38	120.66 (120.36–120.96)	120.29 (119.84–120.74)	0.18	120.65 (120.35–120.96)	120.33 (119.89–120.76)	0.23
BMI (kg/m^2)[a]	15.73 (15.64–15.82)	15.78 (15.61–15.95)	0.61	15.75 (15.65–15.85)	15.73 (15.58–15.87)	0.78	15.76 (15.66–15.86)	15.71 (15.57–15.85)	0.60
Blood oxygen rate (%)[a]	92.77 (92.61–92.93)	92 (92.11–92.68),4	0.03[b]	92.77 (92.60–92.93)	92.5 (92.25–92.75)	0.08	92.76 (92.59–92.93)	92.52 (92.28–92.76)	0.11
IOP (mmHg)[a]	16.1 (15.96–16.24)	15.78 (15.52–16.03)	0.03[b]	16.05 (15.90–16.20)	15.96 (15.74–16.18)	0.50	16.06 (15.91–16.21)	15.94 (15.73–16.16)	0.38
SE (D)[a]	1.04 (1.00–1.09)	1.16 (1.07–1.24)	0.02[b]	1.06 (1.01–1.12)	1.09 (1.01–1.16)	0.64	1.07 (1.01–1.12)	1.08 (1.01–1.15)	0.73

BMI body mass index, *IOP* intraocular pressure, *SE* spherical equivalent.

[a]Mean (95% CI).

[b]$P < 0.05$, included group vs excluded group.
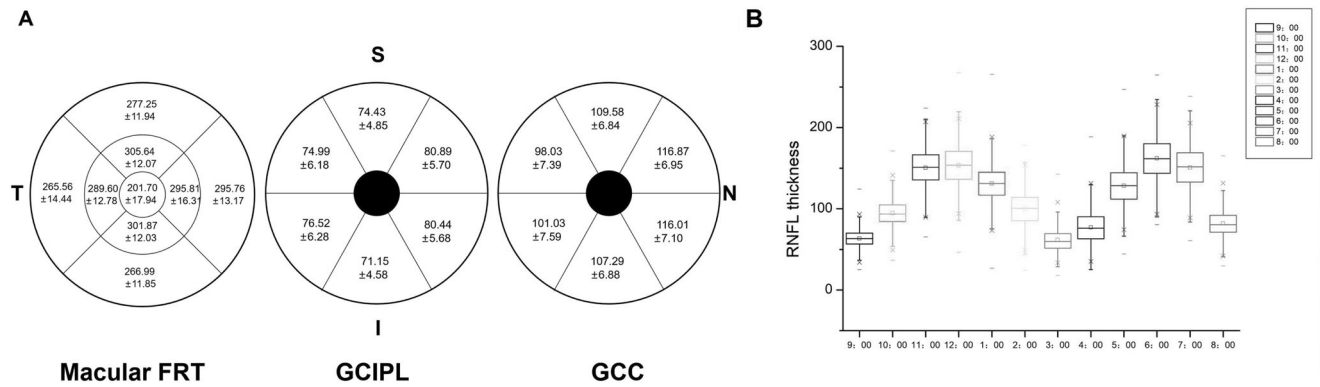
A

Macular FRT   GCIPL   GCC

B

Fig. 2 The average thickness distribution of retina. A Thickness distribution maps of macular layers. Topographic distributions of macular FRT, GCIPL, and GCC thickness in different sectors are shown through the picture. **B** 12 clock-wised sections of cpRNFL thickness distribution. The mean ± SD values (lm) are presented. S superior, I inferior, N nasal, T temporal.

scatter plots and fitted surfaces between RNFL and macular FRT, GCC, GCIPL, and SE. Based on the figures, the retina thickness became thinner with increasing myopia, while an increase in cpRNFL thickness caused an increase in macular FRT, GCC, and GCIPL.

Discussion

This is the first article to comprehensively report the thickness of cpRNFL, GCC, GCIPL, and macular FRT, as well as the optic disc parameters of Tibetan minority children inhabiting the plateau region. LCES employed the wide-field OCT scanning methods to establish a baseline ocular information reference database for grade-1 primary school students. According to the study, GCC and GCIPL thickness were correlated with BMI and IOP in the macular area. However, GCC and GCIPL thickness were not correlated with optical disc indicators. In the same line, all layers of the macula and cpRNFL thickness were found to be positively correlated with SE. In addition, the thickness of each layer of the macula was positively correlated with cpRNFL thickness. Boys and girls had significantly different average RNFL thickness, especially in the inferior and superior regions.

The average macular FRT, GCIPL, and GCC thickness obtained herein were $279.19 \pm 10.61\,\mu m$, $76.41 \pm 4.70\,\mu m$, and $108.15 \pm 6.15\,\mu m$, respectively. Previous studies have reported that nasal region is thinner than the inferior and superior regions of the inner circle while the nasal subregion is the thickest region of the outer circle [14, 21, 22]. These variations in thickness were attributed to the crowding of nerve fibers along with the superior and inferior arcuate bundles as well as along the papillomacular bundle. These results were not consistent with those of Chaglasian et al. [19], who reported a macular FRT, GCIPL, and GCC thickness of $237.079 \pm 20.899\,\mu m$,

$71.363 \pm 5.924\,\mu m$, and $105.949 \pm 8.533\,\mu m$, respectively. The macular FRT herein was also thicker than that obtained in the Sydney Childhood Eye Study (SCES) that employed the stratus OCT method [14]. This was despite both studies having a similar age distribution. The average thickness of cpRNFL herein had a consistent pattern with that of previous ISNT law. Nevertheless, cpRNFL thickness herein was higher than that of other similar studies [16, 17]. This was attributed to several factors. First, the Topcon's clinical research was conducted on adult subjects while LCES was conducted in children. There were differences between the instruments used in variable studies. Some employed stratus OCT while others employed SD-OCT. Moreover, there were differences even between OCT based on SD techniques of different brands. However, the distribution of macular FRT thickness in which the superior region was the thickest in the inner ring while the nasal region was the thickest in the outer ring was consistent with that of previous studies despite different types of OCT being used [23–25]. Herein, one type of OCT will be used continuously during follow-up examinations to obtain comparable data.

The macular FRT, GCIPL, and GCC thickness data in this study were similar to those of a Chinese childhood study with an average age of 11 years. The study reported a thickness of macular FRT, GCIPL, and GCC of $286.25\,\mu m$ without SD, $77.00 \pm 4.78\,\mu m$ and $107.68 \pm 5.95\,\mu m$, respectively [15], In another multi-ethnic Asian study [26], the average GCIPL of the Chinese population (55.2 ± 7.5 years for age) was $82.6 \pm 6.1\,\mu m$. This was significantly higher than that of this study. These studies strongly suggested that the thickness of the macular area decreased with age given that the thickness of macular FRT and GCIPL reported herein were either similar or thicker than those of the two studies whose average age of Chinese subjects was higher than that of this study. This could have also been attributed to the sample of Tibetan children herein as well as to machines and methods used among other factors. In the

Table 2 Demographic and ocular independent variables associated with the thickness of GCIPL GCC and full retinal macula.

Layer	Factors	Unstandardized coefficient	Standardized coefficient	Standard error	P-value	VIF	R^2
Full retinal macula	Intercept	256.18		11.33			0.0334
	Ethnicity	−1.73	−0.04	1.27	0.17	1.01	
	Sex	−0.60	−0.03	0.56	0.29	1.03	
	Age	0.51	0.02	0.66	0.44	1.11	
	Height	0.10	0.05	0.05	0.06	1.12	
	BMI	0.25	0.04	0.16	0.10	1.04	
	Blood oxygen rate	0.07	0.02	0.10	0.50	1.01	
	IOP	−0.13	−0.03	0.10	0.19	1.03	
	SE	1.80	0.15	0.32	<0.001[a]	1.02	
GCIPL	Intercept	69.90		5.00			0.0416
	Ethnicity	0.23	0.01	0.56	0.68	1.01	
	Sex	0.22	0.02	0.25	0.37	1.03	
	Age	0.28	0.03	0.29	0.35	1.11	
	Height	0.00	0.01	0.02	0.85	1.12	
	BMI	0.16	0.06	0.07	0.02[a]	1.04	
	Blood oxygen rate	0.02	0.01	0.04	0.61	1.01	
	IOP	−0.12	−0.07	0.05	0.01[a]	1.03	
	SE	0.90	0.17	0.14	<0.001[a]	1.02	
GCC	Intercept	97.36		6.61			0.0199
	Ethnicity	1.04	0.04	0.74	0.16	1.01	
	Sex	0.33	0.03	0.33	0.32	1.03	
	Age	0.52	0.04	0.39	0.18	1.11	
	Height	0.04	0.04	0.03	0.16	1.12	
	BMI	0.18	0.05	0.09	0.05[a]	1.04	
	Blood oxygen rate	-0.01	−0.00	0.06	0.89	1.01	
	IOP	−0.14	−0.06	0.06	0.02[a]	1.03	
	SE	0.56	0.08	0.19	<0.001[a]	1.02	
cpRNFL	Ethnicity	−0.73	−0.01	1.46	0.62	/	/
	Gender	2.39	0.1	0.66	<0.001[a]		
	Age	1.36	0.05	0.73	0.06		
	Height	0.02	0.01	0.06	0.77		
	BMI	0.2	0.03	0.18	0.28		
	Blood oxygen rate	0.07	0.02	0.12	0.56		
	IOP	−0.15	−0.04	0.12	0.21		
	SE	1.45	0.1	0.39	<0.001[a]		

VIF variance expansion factor.

[a]Independent factors significantly associated with the macular FRT, GCIPL, GCC, cpRNFL thickness in the regression models.

follow-up examinations, more reliable data will be collected and an appropriate answer arrived at because the children will be aging.

Multivariate regression and correlation analyses revealed that GCC and GCIPL thickness were negatively associated with IOP but positively associated with BMI, while no difference was found in macular FRT and cpRNFL. Previous studies have also used BMI as an evaluation index in children although the standards of

BMI in children and adults are different [14, 15, 24, 27]. Different studies reported inconsistent conclusions about the correlations between retinal thickness and the above indicators like BMI and IOP. Cheng et al. [15], reported that there was no relevance between GCIPL, GCC, BMI, and IOP. However, Diniz-Filho et al. [28], reported that high levels of IOP accelerated the rate of RNFL thinning over time. Nevertheless, further research is needed to confirm whether the increase of IOP and the decrease of
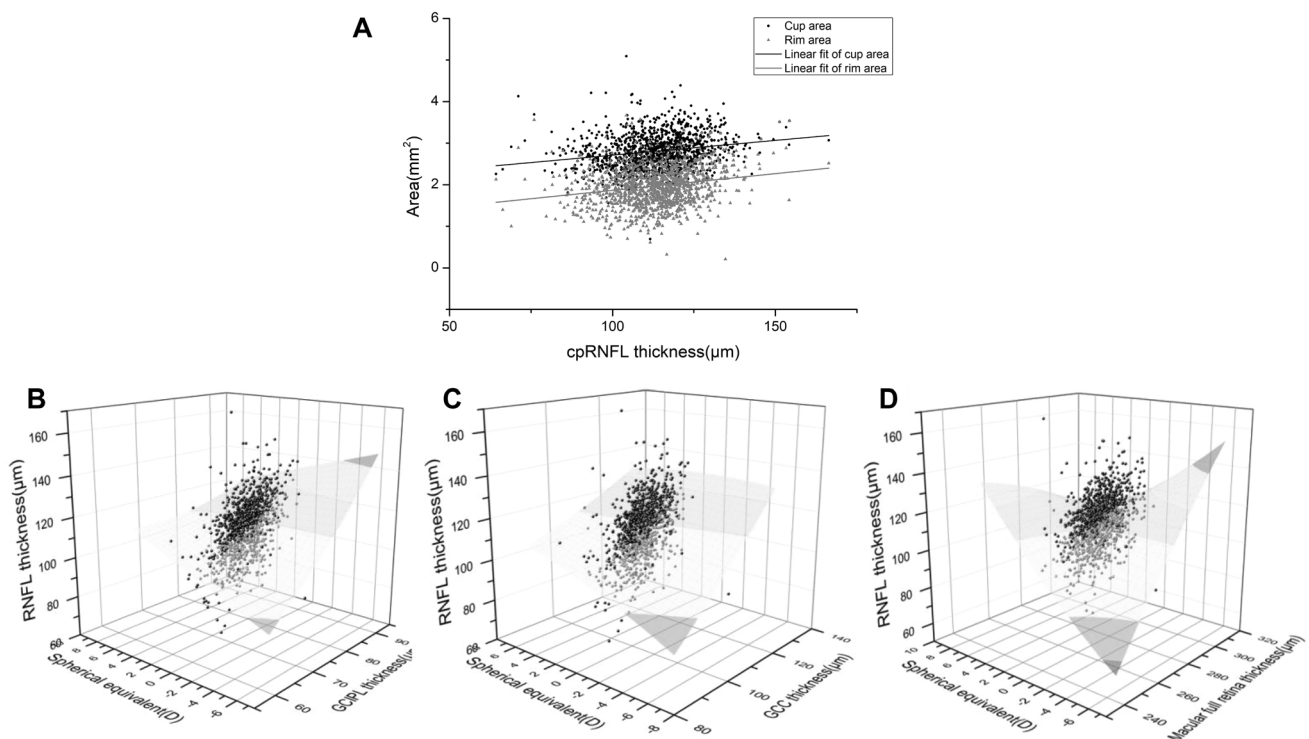
Fig. 3 Correlation between cpRNFL thickness and other retinal parameters. A Scattergrams showing the relationship of average cpRNFL thickness in right eyes with cup area and rim area. **B** 3D scatter plots showing the relationships of cpRNFL thickness with SE and GCIPL thickness; **C** the relationships of cpRNFL thickness with SE and GCC thickness; **D** the relationships of cpRNFL thickness with SE and macular FRT.

BMI can be used as indicators to predict the thickness of GCIPL and GCC.

After correcting systemic and ocular factors, the average cpRNFL thickness in the inferior and superior regions was thicker in girls than in boys. However, there were no significant differences in macular FRT, GCC, and GCIPL between the boys and the girls. Previous studies involving Chinese children and adults reported that there were significant differences in RNFL thickness between males and females [27, 29–31]. There were boys whose macula FRT was thicker than that of girls in all regions of the inner ring despite the average FRT of the macula not being related to gender. This result was consistent with that of other studies [14, 15, 20, 23]. Herein, differences in the average thickness of cpRNFL between boys and girls were not significant (2.32 μm thicker in girls). The thickness of cpRNFL was affected by the covered blood vessels of the optic disc [25]. Nonetheless, the correlation between gender and retinal thickness needs to be further explored in the subsequent examinations.

RNFL thickness may be ethnic specific [32, 33]. Herein, Tibetan minority children were recruited. The children lived in high altitudes of Tibet characterized by long hours of sunshine and low oxygen concentrations. Despite this, there was no correlation between cpRNFL thickness and ethnicity

as well as between macular FRT, GCC, and GCIPL thickness and ethnicity. There was also no correlation between ethnicity and blood oxygen saturation even for the Han majority children. However, these results were not consistent with those of other studies involving Caucasian [23, 32] and Chinese Han [24] children of the same age group. Compared with these studies, the average RNFL thickness herein was significantly higher, especially in the inferior and superior quadrants. The underlying mechanism is supposed to be the prolonged light exposure time which may slow the growth of the axial length thus affect the eye development in the previous study [34]. Herein, the lack of any correlation of RNFL thickness to sunlight exposure was attributed to the small sample size which was insufficient for differential analysis. Cognizant to this, the effects of sunlight exposure time and oxygen concentration on the thickness of RNFL in Tibetan children should be observed and explored in subsequent examinations and studies.

The average macular FRT, GCIPL, GCC, and cpRNFL thickness had a positive correlation with the SE value. As such, the retina thickness decreased as the refractive error degree decreased, consistent with previous studies [17, 23–25, 27]. Similarly, RNFL thickness was positively correlated with the optic disc area, rim area, as well as with the macular FRT, GCIPL, and GCC thickness. These results

were consistent with those previous studies based on the physiology structure composition [15, 19, 35–37].

Despite this study having unquestionable strengths such as having a large unbiased sample, a school-based design, a specific ethnic group, standardized examination, comprehensive OCT data, and detailed analyses, it was limited by several factors. The axial length data was not collected and thus correlations could not be made during statistical correlation analysis. The influence of ethnic factors on retinal thickness could not be fully discussed because of the small sample size of children from Han and other ethnic groups. The cooperation of children with OCT detection was not well enhanced.

Evidently, SD-OCT was successfully used to obtain comprehensive ocular data of Tibetan minority children. The findings of this study contribute to the establishment of a normative ophthalmology database of Tibetan children. The study further confirms that OCT can be successfully used for the diagnosis of ophthalmic disorders during long-term diagnosis and monitoring in plateau area in China.

Summary

What was known before

- Vision screening for children is fundamental to detect reduced visual acuity and risk factors that threaten vision impairment or blindness around the world.
- A combined series of screening methods, including objective and quantified measurements, of visual function and structure changes with high accuracy and reliability, were identified as substantial benefits for children's ocular health assessment.
- Most previous studies were limited to observing only a particular region of the retina, such as the optic disc or macular area.

What this study adds

- This manuscript summarizes the normal thickness distribution of macular retina, ganglion cell-inner plexiform layer (GCIPL), ganglion cell complex (GCC), circumpapillary retina nerve fiber layer (cpRNFL), and optic disc parameters in first-year Tibetan children in Lhasa.
- We took the advantages of wide-field OCT scanning methods which cover the macula and optic disc area to establish a baseline and reference database for grade-1 primary school students and will continue to follow-up for 5 years.

Author contributions JF and WC initiated the study design. WC, YY, WD, and HS prepared the consent form. All authors were involved in the research process and data collation. LL assisted in the collation and analysis of the data. YY and JF drafted and finalized the study protocol. All authors reviewed the study protocol and approved the final manuscript.

Compliance with ethical standards

Conflict of interest The authors declare that they have no conflict of interest.

References

1. Solebo AL, Teoh L, Rahi J. Epidemiology of blindness in children. Arch Dis Child. 2017;102:853–7.
2. Loh AR, Chiang MF. Pediatric vision screening. Pediatrics Rev. 2018;39:225–34.
3. Adhi M, Duker JS. Optical coherence tomography-current and future applications. Curr Opin Ophthalmol. 2013;24:213–21.
4. Gupta S, Zivadinov R, Ramanathan M, Weinstock-Guttman B. Optical coherence tomography and neurodegeneration: are eyes the windows to the brain? Expert Rev neurotherapeutics. 2016;16:765–75.
5. Petzold A, Balcer LJ, Calabresi PA, Costello F, Frohman TC, Frohman EM, et al. Retinal layer segmentation in multiple sclerosis: a systematic review and meta-analysis. Lancet Neurol. 2017;16:797–812.
6. Wang N, Xu X, Zou H, Zhu J, Wang W, Ho PC. The status of diabetic retinopathy and diabetic macular edema in patients with type 2 diabetes: a survey from Beixinjing District of Shanghai city in China. Ophthalmologica. 2008;222:32–36.
7. Wirtitsch MG, Ergun E, Hermann B, Unterhuber A, Stur M, Scholda C, et al. Ultrahigh resolution optical coherence tomography in macular dystrophy. Am J Ophthalmol. 2005;140:976–83.
8. Markomichelakis NN, Halkiadakis I, Pantelia E, Peponis V, Patelis A, Theodossiadis P, et al. Patterns of macular edema in patients with uveitis: qualitative and quantitative assessment using optical coherence tomography. Ophthalmology. 2004;111: 946–53.
9. Gu S, Glaug N, Cnaan A, Packer RJ, Avery RA. Ganglion cell layer-inner plexiform layer thickness and vision loss in young children with optic pathway gliomas. Invest Ophthalmol Vis Sci. 2014;55:1402–8.
10. Inuzuka H, Sawada A, Yamamoto T. Comparison of changes in macular ganglion cell-inner plexiform layer thickness between medically and surgically treated eyes with advanced glaucoma. Am J Ophthalmol. 2018;187:43–50.

11. Zhang X, Dastiridou A, Francis BA, Tan O, Varma R, Greenfield DS, et al. Baseline Fourier-domain optical coherence tomography structural risk factors for visual field progression in the advanced imaging for glaucoma study. Am J Ophthalmol. 2016;172: 94–103.

12. Hered RW. Effective vision screening of young children in the pediatric office. Pediatr Ann. 2011;40:76–82.

13. Virgili G, Menchini F, Dimastrogiovanni AF, Rapizzi E, Menchini U, Bandello F, et al. Optical coherence tomography versus stereoscopic fundus photography or biomicroscopy for diagnosing diabetic macular edema: a systematic review. Invest Ophthalmol Vis Sci. 2007;48:4963–73.

14. Huynh SC, Wang XY, Rochtchina E, Mitchell P. Distribution of macular thickness by optical coherence tomography: findings from a population-based study of 6-year-old children. Invest Ophthalmol Vis Sci. 2006;47:2351–7.

15. Cheng L, Wang M, Deng J, Lv M, Jiang W, Xiong S, et al. Macular ganglion cell-inner plexiform layer, ganglion cell complex, and outer retinal layer thicknesses in a large cohort of Chinese children. Invest Ophthalmol Vis Sci. 2019;60:4792–802.

16. Leung MM, Huang RY, Lam AK. Retinal nerve fiber layer thickness in normal Hong Kong chinese children measured with optical coherence tomography. J Glaucoma. 2010;19:95–99.

17. Qian J, Wang W, Zhang X, Wang F, Jiang Y, Wang W, et al. Optical coherence tomography measurements of retinal nerve fiber layer thickness in chinese children and teenagers. J Glaucoma. 2011;20:509–13.

18. Dichtl A, Jonas JB, Naumann GO. Retinal nerve fiber layer thickness in human eyes. Graefe's Arch Clin Exp Ophthalmol. 1999;237:474–9.

19. Chaglasian M, Fingeret M, Davey PG, Huang WC, Leung D, Ng E, et al. The development of a reference database with the Topcon 3D OCT-1 Maestro. Clin Ophthalmol. 2018;12:849–57.

20. Duan XR, Liang YB, Friedman DS, Sun LP, Wong TY, Tao QS, et al. Normal macular thickness measurements using optical coherence tomography in healthy eyes of adult Chinese persons: the Handan Eye Study. Ophthalmology. 2010;117:1585–94.

21. Landau D, Schneidman EM, Jacobovitz T, Rozenman Y. Quantitative in vivo retinal thickness measurements in healthy subjects. Ophthalmology. 1997;104:639–42.

22. Zeimer R, Shahidi M, Mori M, Zou S, Asrani S. A new method for rapid mapping of the retinal thickness at the posterior pole. Invest Ophthalmol Vis Sci. 1996;37:1994–2001.

23. Huynh SC, Wang XY, Burlutsky G, Rochtchina E, Stapleton F, Mitchell P. Retinal and optic disc findings in adolescence: a population-based OCT study. Invest Ophthalmol Vis Sci. 2008;49:4328–35.

24. Kang MT, Li SM, Li H, Li L, Li SY, Zhu BD, et al. Peripapillary retinal nerve fibre layer thickness and its association with refractive error in Chinese children: the Anyang Childhood Eye Study. Clin Exp Ophthalmol. 2016;44:701–9.

25. Huynh SC, Wang XY, Rochtchina E, Mitchell P. Peripapillary retinal nerve fiber layer thickness in a population of 6-year-old children: findings by optical coherence tomography. Ophthalmology. 2006;113:1583–92.

26. Tham YC, Chee ML, Dai W, Lim ZW, Majithia S, Siantar R, et al. Profiles of Ganglion Cell-Inner Plexiform Layer Thickness in a Multi-Ethnic Asian Population: The Singapore Epidemiology of Eye Diseases Study. Ophthalmology. 2020;127:1064–76.

27. Wang CY, Zheng YF, Liu B, Meng ZW, Hong F, Wang XX, et al. Retinal nerve fiber layer thickness in children: The Gobi Desert Children Eye Study. Invest Ophthalmol Vis Sci. 2018;59:5285–91.

28. Diniz-Filho A, Abe RY, Zangwill LM, Gracitelli CP, Weinreb RN, Girkin CA, et al. Association between intraocular pressure and rates of retinal nerve fiber layer loss measured by optical coherence tomography. Ophthalmology. 2016;123:2058–65.

29. Chen L, Huang J, Zou H, Xue W, Ma Y, He X, et al. Retinal nerve fiber layer thickness in normal Chinese students aged 6 to 17 years. Invest Ophthalmol Vis Sci. 2013;54:7990–7.

30. Zhao L, Wang Y, Chen CX, Xu L, Jonas JB. Retinal nerve fibre layer thickness measured by Spectralis spectral-domain optical coherence tomography: The Beijing Eye Study. Acta Ophthalmol. 2014;92:e35–41.

31. Zhu BD, Li SM, Li H, Liu LR, Wang Y, Yang Z, et al. Retinal nerve fiber layer thickness in a population of 12-year-old children in central China measured by iVue-100 spectral-domain optical coherence tomography: the Anyang Childhood Eye Study. Invest Ophthalmol Vis Sci. 2013;54:8104–11.

32. Samarawickrama C, Wang JJ, Huynh SC, Pai A, Burlutsky G, Rose KA, et al. Ethnic differences in optic nerve head and retinal nerve fibre layer thickness parameters in children. Br J Ophthalmol. 2010;94:871–6.

33. Ho H, Tham YC, Chee ML, Shi Y, Tan NYQ, Wong KH, et al. Retinal nerve fiber layer thickness in a multiethnic normal asian population: the singapore epidemiology of eye diseases study. Ophthalmology. 2019;126:702–11.

34. Read SA, Collins MJ, Vincent SJ. Light exposure and eye growth in childhood. Invest Ophthalmol Vis Sci. 2015;56:6779–87.

35. Mwanza JC, Durbin MK, Budenz DL, Girkin CA, Leung CK, Liebmann JM, et al. Profile and predictors of normal ganglion cell-inner plexiform layer thickness measured with frequency-domain optical coherence tomography. Invest Ophthalmol Vis Sci. 2011;52:7872–9.

36. Demirkaya N, van Dijk HW, van Schuppen SM, Abràmoff MD, Garvin MK, Sonka M, et al. Effect of age on individual retinal layer thickness in normal eyes as measured with spectral-domain optical coherence tomography. Invest Ophthalmol Vis Sci. 2013;54:4934–40.

37. Blum Meirovitch S, Leibovitch I, Kesler A, Varssano D, Rosenblatt A, Neudorfer M. Retina and nerve fiber layer thickness in eyes with thyroid-associated ophthalmopathy. Isr Med Assoc J. 2017;19:277–81.